

Influence of External Cables on EM Exposure Investigated with a Human Model in a 3T MRI Coil

M. Kozlov, N. Weiskopf and H.E. Möller

Max Planck Institute for Human Cognitive and Brain Sciences

Leipzig, Saxony, Germany

kozlov@cbs.mpg.de, weiskopf@cbs.mpg.de, moeller@cbs.mpg.de

Abstract—We evaluated the influence of a commercial clip-on magnetic field camera with 16 field probes on electromagnetic exposure employing a human model located in a realistic 3T MRI whole body radio frequency (RF) coil. The camera setup had a relevant impact on the electric and magnetic field distribution. Variety of generated electric field depended on usage of RF cable traps.

I. INTRODUCTION

To get optimal performance of magnetic resonance imaging (MRI) some experimental setups include additional monitoring tools located in the scanner bore, such as a clip-on magnetic field camera (Skope Magnetic Resonance Technologies AG, Zurich, Switzerland). The camera measures the encoding field dynamics during the MR acquisition. In case of head MRI, the camera setup consists of 16 field probes that are in close proximity to human head and 16 cables connecting the probes to an electronic box. The probes and cables are located inside the MRI radio frequency (RF) transmitter coil and are in proximity to the coil. The camera setup operates as a set of antennas, the resonance performance of which depends on the relative positioning of the probes, cables and human body, as well as the quality of RF cable traps that block stray RF current from flowing on cable shields. This set of antennas can modify the electromagnetic (EM) field inside human body that may, in principle, impact the operation of the MR scanner's RF safety supervision system.

II. METHODS

We investigated the RF field modification from a Skope clip-on camera located in a 123.2 MHz 32-rung high-pass whole-body birdcage coil of the customized Siemens 3T Connectom scanner, which is a modified 3T MAGNETOM Skyra system (Siemens Healthineers, Erlangen, Germany). The scanner inner bore diameter was 555 mm; total coil length was 450 mm. Two RF sources were used to excite the coil for both feeds with identical amplitudes of 1 W and a 90° phase shift as in quadrature excitation. Electrical components (fixed and variable capacitors, RF feed sub-circuit) were connected across 3-mm ring gaps centered between each two adjacent rungs. The coil was loaded with a human head and torso model [1] located at head land mark position (Fig. 1). The coil was tuned using RF-circuit (ADS 2016, Keysight, Santa Rosa, CA, USA) and 3D EM (HFSS 2014, ANSYS, Canonsburg, PA, USA) co-simulation based approach outlined in [2].

Components of the clip-on camera were modelled as: field probes as oval copper case (length 57 mm, major radius 23 mm, minor radius 8 mm), cables as copper wire of 2 mm in

diameter and approximately 60 cm length, electronic box as a rectangular copper box with dimensions: 240×140×200 mm³, and cable traps as 10 kΩ resistors connected across a wire gap located 10 mm from the copper box. The spatial distribution of Skope field probes was similar to the distribution proposed in installation document. Spatial cable trajectories were similar to the trajectories of the experimental setup.

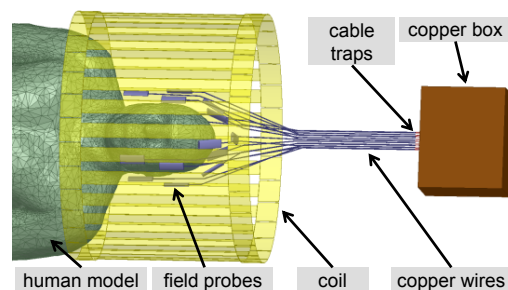


Fig. 1. Birdcage coil loaded with human model and field measurement setup.

To evaluate influence of the Skope clip-on camera, three simulations were performed: (i) the human model only, (ii) the human model with numerical setup of the camera but without the cable traps, and (iii) the human model with full numerical setup of the camera.

III. RESULTS AND DISCUSSION

Results obtained without consideration of the camera setup were consistent with the literature [3]: the transverse magnetic field magnetic field component (B_{1+}) with clockwise circular polarization was rather homogeneously distributed across the head and the power deposition showed a maximum in the neck region (Fig. 2). The camera setup significantly modified the EM field distribution (Figs. 3-5) and the ratio of the power deposited in human head to power deposited in entire model. The camera setup without the cable traps resulted in 12% decrease B_{1+} at iso-center compared to the human model only result (Table I). An inclusion of the cable traps in the numerical domain resulted in 20% increase of B_{1+} at iso-center. The total power deposited in the human model was not affected by the camera setup and the cable traps.

TABLE I. RESULT SUMMARY

| Numerical setup | Power in human model, W | Power in human head, W | B_{1+} at iso-center, μT | B_{1-} at iso-center, μT |
|------------------------------------|-------------------------|------------------------|---------------------------------|---------------------------------|
| human model | 0.963 | 0.38 | 0.488 | 0.12 |
| human model + camera | 0.968 | 0.34 | 0.432 | 0.07 |
| human model + camera + cable traps | 0.981 | 0.49 | 0.584 | 0.12 |

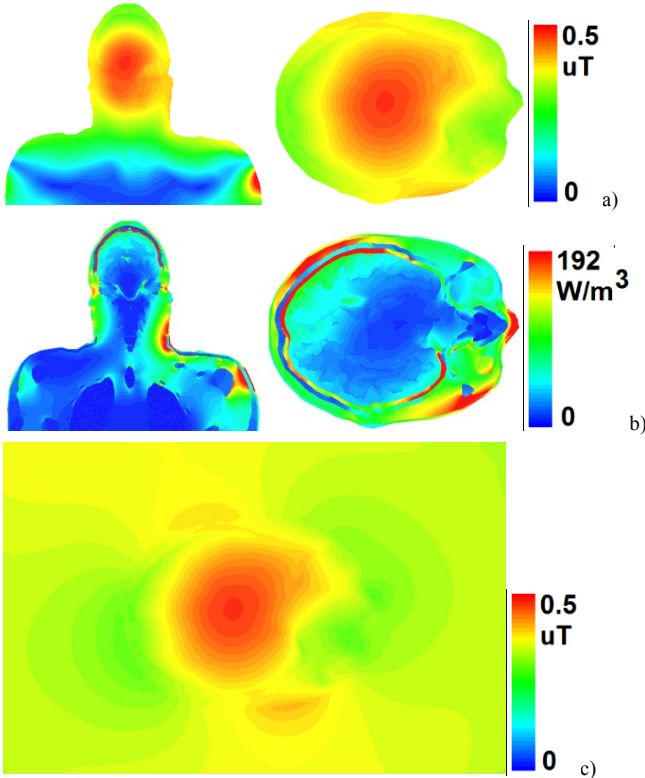


Fig. 2. Results for human model only. (a) Coronal and axial iso-center B_{1+} profiles. (b) Coronal and axial iso-center volume loss density profiles. (c) Axial iso-center B_{1+} slice

Our simulations provide evidence that the magnetic field camera has an impact on the EM field distribution inside and outside a human model located in a commercial 3T whole-body birdcage coil. The observed field variation cannot be readily generalized because only a single spatial distribution of the camera components was included in our investigation. The parameter matrix for this spatial distribution is already quite large. Considering that typical biological differences between patients undergoing MRI examinations, the total parameter matrix should also include a variety of human models. Although computational power is increasing constantly, it remains a challenge to perform ~ 1000 3D EM simulations of an MRI coil loaded with a human model and the camera setup.

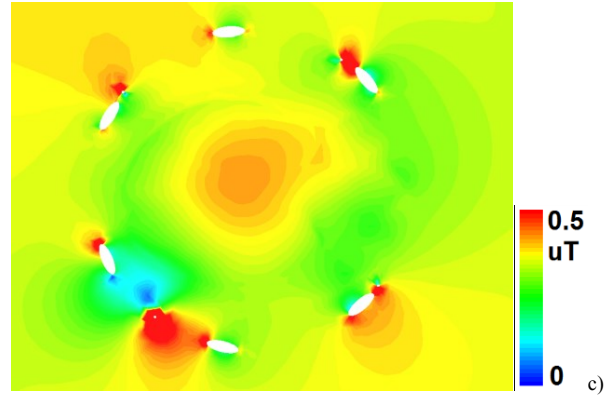
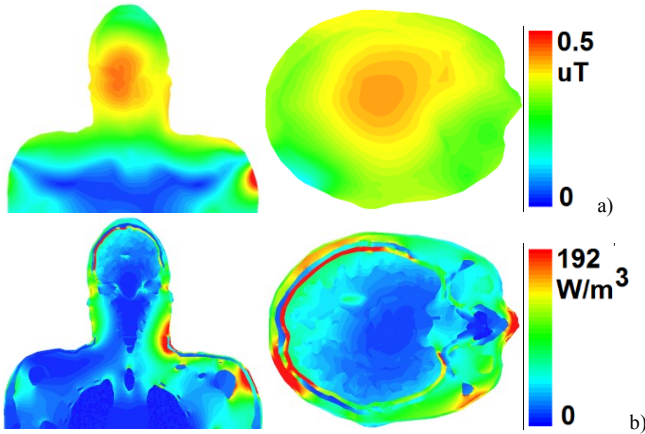


Fig. 3. Results for human model and numerical setup of the camera but without the cable traps. (a) Coronal and axial iso-center B_{1+} profiles. (b) Coronal and axial iso-center volume loss density profiles. (c) Axial iso-center B_{1+} slice included the human model and field probes.

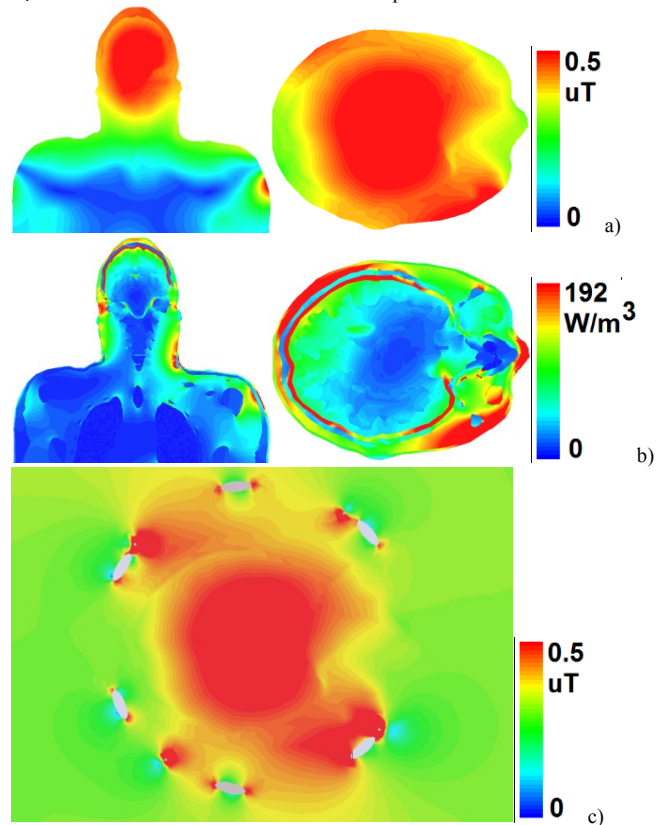


Fig. 4. Results full setup. (a) Coronal and axial iso-center B_{1+} profiles. (b) Coronal and axial iso-center volume loss density profiles. (c) Axial iso-center B_{1+} slice included the human model and field probes.

REFERENCES

- [1] M. Kozlov et al., "Building a High Resolution Surface-Based Human Head and Torso Model for Evaluation of Specific Absorption Rates in MRI", Proceedings of COMCAS 2017; Tel-Aviv, Isreal; 2017; pp. 1-6.
- [2] M. Kozlov et al., "RF Safety of Transcranial Direct Current Stimulation Equipment during MRI", Proceedings of ISMRM 2018, p. 4061.
- [3] D. Yeo et al., "Local Specific Absorption Rate in High-Pass Birdcage and Transverse Electromagnetic Body Coils for Multiple Human Body Models in Clinical Landmark Positions at 3T," J. Magn. Reson. Imag., 33, 2011, pp.1209–1217.